Chemical Engineering Journal 245 (2014) 34–40

Contents lists available at ScienceDirect

Chemical Engineering Journal

journal homepage: www.elsevier.com/locate/cej

# Removal of mercury (II) and chromium (VI) from wastewater using a new and effective composite: Pumice-supported nanoscale zero-valent iron

Tingyi Liu [a], Zhong-Liang Wang [a,b,*], Xiaoxing Yan [a], Bing Zhang [a]

[a] Tianjin Key Laboratory of Water Resources and Environment, Tianjin Normal University, Tianjin 300387, China
[b] State Key Laboratory of Environmental Geochemistry, Institute of Geochemistry, Chinese Academy of Sciences, Guiyang 550002, China

## HIGHLIGHTS

- The properties of NZVI were obviously enhanced using pumice as the support.
- P-NZVI was more effective to remove heavy metals from wastewater.
- P-NZVI is a regenerated material.
- P-NZVI was suitable for applications to *in situ* environmental remediation.

## ARTICLE INFO

*Article history:*
Received 13 January 2014
Received in revised form 31 January 2014
Accepted 3 February 2014
Available online 12 February 2014

*Keywords:*
Pumice
Nanoscale zero-valent iron
Chromium (VI)
Mercury (II)

## ABSTRACT

Nanoscale zero-valent iron successfully supported on pumice (P-NZVI) was used to remove heavy metals from wastewater with a higher removal capacity and efficiency. NZVI particles with a mean diameter of 30.6 nm are distributed uniformly on the surface of P-NZVI. The thermal stability and mechanical strength of P-NZVI were also obviously enhanced. P-NZVI with a 7.7% NZVI mass fraction had a specific surface area ($S_{BET}$) of 32.2 $m^2$/g. The removal capacity of Hg (II) and Cr (VI) by P-NZVI was 332.4 mg Hg/g Fe and 306.6 mg Cr/g Fe, respectively. As an increase of pH, the removal rates of Hg (II) increased but those of Cr (VI) decreased gradually. P-NZVI is a regenerated material. The X-ray photoelectron spectroscope analysis (XPS) results indicated that Hg (II) and Cr (VI) were removed by a rapid physical adsorption in the first 0.5 min and predominantly by reduction. In terms of the efficiency and speed, P-NZVI was a promising candidate for applications to *in situ* environmental remediation, especially to the heavy metals pollution incidents with an extremely high concentration of heavy metals.



## 1. Introduction

Mercury (II) and chromium (VI) are two toxic metals found in various industrial wastewaters. Several industrial activities, such as electroplating, leather tanning, metal finishing and petroleum refining, can cause water pollution by these ions [1,2]. Their levels in the wastewater are much higher than the action level of 0.001 mg/L for Hg (II) and 0.1 mg/L for Cr (VI) [3]. Mercury (II) and chromium (VI) contaminate the environment, affect aquatic life and cause several health problems. Hence, these heavy metals must be removed from wastewaters before being discharged to the environment.

Various methods, including chemical precipitation, membrane filtration, ion exchange and adsorption, were used to remove heavy metals from wastewaters [4]. Recently, the use of nanoscale zero-valent iron (NZVI) to remove heavy metals has become one of the most promising and effective remediation technologies because of its extremely small particle size, large surface area and high reactivity [5–7]. However, NZVI was usually agglomerated in conventional systems along with a decrease of its reactivity and mechanical strength, which limited the practical application of NZVI [8]. In recent years, porous materials, including zeolite, kaolinite, bentonite and pillared clay, have been widely used as mechanical supports to enhance the dispersibility of NZVI particles [9–11]. More recently, NZVI was stabilized by chitosan and supported by chitosan beads to increase the dispersibility and stability

* Corresponding author at: Tianjin Key Laboratory of Water Resources and Environment, Tianjin Normal University, Tianjin 300387, China. Tel./fax: +86 22 23766256.
*E-mail address:* wangzhongliang@vip.skleg.cn (Z.-L. Wang).

http://dx.doi.org/10.1016/j.cej.2014.02.011
1385-8947/

in air [12–14]. Nevertheless, the mechanical strength of chitosan beads needed to be improved [15].

Pumice is a porous volcanic rock and has a large surface area and skeleton structure, which contains open channels allowing water and ions to travel into and out of the crystal structure [16]. Furthermore, pumice can be processed easily and used as a low-cost heavy metals adsorbent [17]. Pumice–iron granular mixtures perform well in removing contaminants and maintaining the long-term hydraulic conductivity [18]. However, only a few studies have focused on using the pumice as the support material for NZVI.

In the study, in order to enhance its dispersibility and stability in the air, NZVI was supported on pumice (P-NZVI) for the removal of Hg (II) and Cr (VI) from aqueous solution. The main objectives are to: (1) synthesize and characterize the new and stable P-NZVI composite, (2) evaluate the removal efficiency of Hg (II) and Cr (VI) by P-NZVI under different experimental conditions, (3) assess the reuse of P-NZVI and (4) test the role of pumice during remediation process and investigate the elemental composition of final products to reasonably conclude the removal mechanism of Hg (II) and Cr (VI) by P-NZVI.

## 2. Materials and methods

### 2.1. Materials and chemicals

Pumice with a diameter of 0.5–1.0 mm was provided by Dahe Building Materials Co., Ltd. (Hebei, China) and the chemical composition was 67.2% $SiO_2$, 22.1% $Al_2O_3$, 2.98% $Fe_2O_3$, 2.28% CaO and small amounts of Mn, Mg, P and S. Iron (III) chloride hexahydrate ($FeCl_3{\cdot}6H_2O$) and sodium borohydride ($NaBH_4$) were purchased from Fuchen Chemical Reagent Manufactory (Tianjin, China). $K_2CrO_4$, $HgCl_2$ and absolute alcohol were provided by First Chemical Reagent Manufactory (Tianjin, China). All other chemicals were of analytical grade purity.

### 2.2. Preparation of P-NZVI

Pumice-supported nanoscale zero-valent iron (P-NZVI) was prepared using conventional liquid-phase methods via the reduction of ferric ion ($FeCl_3{\cdot}6H_2O$) by borohydride ($NaBH_4$) and pumice was used as a support material [7,10,19]. Pumice (3.36 g) was initially placed into a three-necked open flask. A ferric solution prepared by dissolving ferric chloride hexahydrate (1.35 g) in an ethanol water solution (100 mL, 8:1 v/v) was added into the flask. The previous mixture was stirred for 1 h. Subsequently, a freshly prepared $NaBH_4$ solution (0.95 g of $NaBH_4$ in 100 mL deionized water) was added drop-wise into the mixture at a rate of 50–60 drops per minute with constant stirring for 60 min after addition. Every 10 min, the mixture was dispersed by sonication for 2 min operating at 40 kHz. The theoretical mass fraction of NZVI in prepared P-NZVI was about 7.7%. The synthesized materials were separated from the liquid solution via the magnet and dried at 65 °C overnight. P-NZVI was stored in brown and sealed bottles for further use. The whole process was carried out in a nitrogen atmosphere.

### 2.3. Batch experiments

Batch experiments for removal of Hg (II) and Cr (VI) were carried out in polytetrafluoroethylene bottles at room temperature using the mechanical agitation. To each bottle, 100 mL Hg (II) and Cr (VI) (60 mg/L) solution and P-NZVI were added. Sampling was made at a certain time-interval and the samples were filtered through a 0.42 μm filter. All experiments were performed in duplicate.

### 2.4. Characterization and analytical methods

The concentrations of Hg (II) and Cr (VI) in the solution were measured using an inductively coupled plasma-mass spectrometry (ICP-MS, Elan-9000, PE). The P-NZVI samples were collected after reacting with wastewater for 0.5, 1, 2, 10, and 60 min, respectively, and used to the X-ray photoelectron spectroscope analysis (XPS, PHI 5000 Versa Probe). The specific surface area ($S_{BET}$) of P-NZVI was measured by the Brunauer–Emmett–Teller (BET) $N_2$ method. The thermal stability of P-NZVI was determined using a thermogravimetric analyzer (TGA-Q500, Switzerland). The morphological analysis of NZVI was performed using a transmission electron microscope (TEM, FEI Tecnai G2 F20). The morphological analysis of P-NZVI was performed using a scanning electron microscope (SEM) with an energy-dispersive X-ray spectrometer (EDS) (SEM/EDS, FEI Nova NanoSEM 230).

## 3. Results and discussion

### 3.1. Characterization of P-NZVI

The morphology of P-NZVI is presented in Fig. 1. It can be seen from Fig. 1(a) that pumice is porous with open channels and rugged surfaces [16], which is favorable for the load and support of NZVI particles on overall framework and all of its surfaces. Other researchers reported that pumice particles consisted of a network of irregular or oval shape internal voids/pores or vesicles, some of which were interconnected and open to the external surface [20]. Pumice was a promising porous support for the immobilization of $TiO_2$ used for the removal of pollutants from aqueous solutions [21,22]. NZVI particles are distributed uniformly on the surface of pumice, indicating that pumice as a support material can prevent NZVI particles from agglomeration (Fig. 1(b)). Pumice is highly abrasive and porous with the pore volumes up to 85% [23], which indicates that pumice is suitable for supporting NZVI. Pumice stones were excellent solid supports in biological fluidized-bed reactors with the low energy consumption [24]. NZVI particles are nearly spherical in shape and uniform in size with a mean diameter of 30.6 nm (Fig. 1(c)). The dispersed distribution of NZVI particles can also be found in Fig. 1(c), which demonstrates again that pumice is effective to enhance the dispersibility of NZVI particles. Other porous materials, such as zeolite, kaolinite, bentonite and chitosan beads, were also useful to enhance the dispersibility of NZVI particles [7,9,10,25].

Surface chemistry of pumice played an important role in removing of pollutants from wastewater [26]. In order to better understand the rough surface of P-NZVI, EDS survey for P-NZVI marked with "+" in Fig. 1(b) was conducted. The EDS result showed that P-NZVI mainly consisted of Fe, O, C, Si, Mg, Ca, K, Na, Al and Au, and no notable peaks of other elements were observed (Fig. 1(d)). Iron came from NZVI. The O, C, Si, Mg, Ca, K, Na and Al would come from pumice. The Au would be introduced when SEM samples were prepared. Chemical composition of pumice powder was 74% of $SiO_2$, 15.6% of $Al_2O_3$, 6.1% of $Na_2O$ and 2.4% of $K_2O$, and the large proportion of free silica sites at the surface resulted in a negatively charged surface [16]. However, uncoated Kay and Nev pumice had $pH_{pzc}$ values in the neutral range [23].

The $S_{BET}$ of pumice and NZVI was 9.6 and 60.8 $m^2/g$, respectively. P-NZVI with a 7.7% NZVI mass fraction had a $S_{BET}$ of 32.2 $m^2/g$. K-NZVI with a 20% NZVI mass fraction and B-NZVI with a 50% NZVI mass content had a $S_{BET}$ of 26.11 and 39.94 $m^2/g$, respectively, which were used to remove heavy metals from wastewater with high efficiencies [7,27]. So it can be predicted that P-NZVI prepared in the study will be useful to remove heavy metals from aqueous solutions.

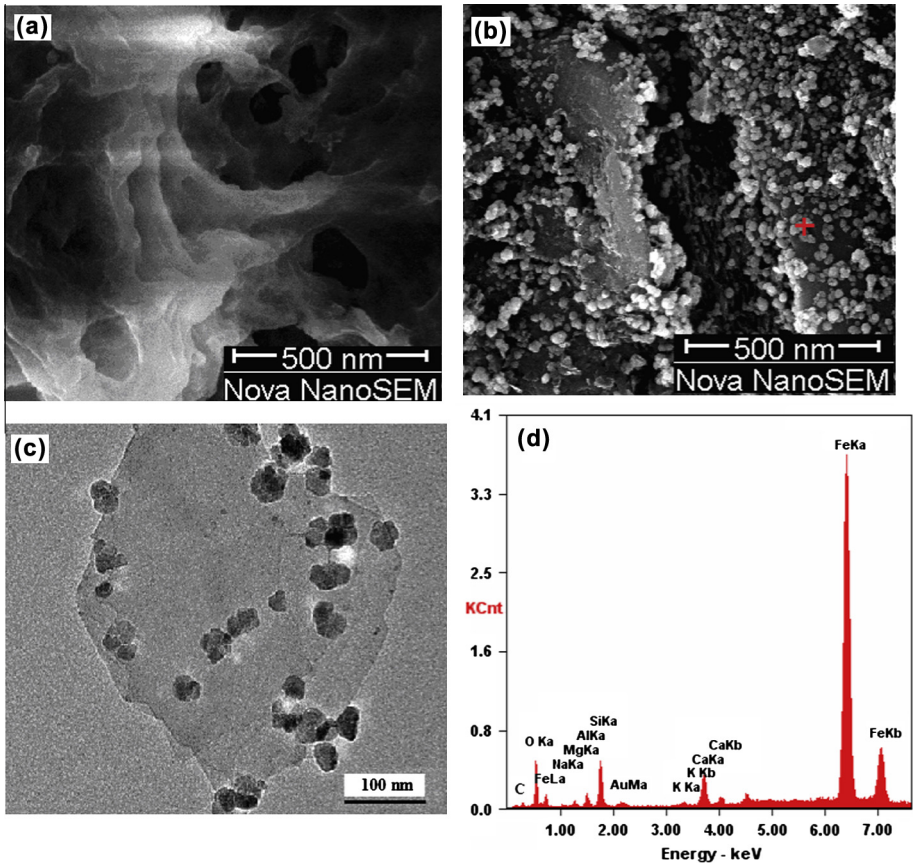


**Fig. 1.** The morphology of P-NZVI was analyzed: (a) SEM image of pumice, (b) SEM of P-NZVI, (c) TEM image of NZVI and (d) EDS survey for P-NZVI marked with "+" in (b).

### 3.2. The thermal stability of P-NZVI

The TG curve of P-NZVI from 15 to 550 °C is shown in Fig. 2. It shows a first thermal event in the range 15–150 °C, which corresponds to a mass loss of approximately 1.3% (Fig. 2). This loss is attributed to the evaporation of water remaining in the pore of P-NZVI. The TG curve is stable in the range of 150–550 °C, which indicates that there are few changes in the mass loss of P-NZVI. A result can be concluded that the thermal stability of P-NZVI is good below 550 °C. Thermal stability of ECH–CS–NZVI beads is enhanced after ECH cross-linking with CS–NZVI beads [14]. However, the thermal stability of P-NZVI is better than that of ECH–CS–NZVI.

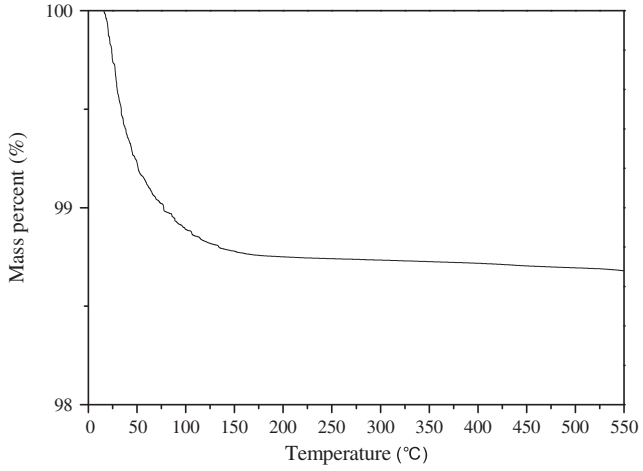


**Fig. 2.** TG curve of P-NZVI in the range 15–550 °C.

### 3.3. Mechanical properties of P-NZVI

Mechanical strength of ECH–CS–NZVI beads and P-NZVI were determined following a previously reported method [28]. The results are shown in Table 1. It can be seen from Table 1 that crumpling ratios of P-NZVI are markedly reduced by comparison with ECH–CS–NZVI beads. It indicates that the mechanical strength of P-NZVI is obviously enhanced using pumice as the support material, which is contributed by the hard properties of pumice stone [23]. As a result, the stuffed phenomenon caused by the scratched beads [25] may be avoided when P-NZVI is used as the reactive materials in permeable reactive barriers.

### 3.4. Effect of initial concentrations of heavy metals

The effect of initial concentrations of heavy metals was estimated and the result is shown in Fig. 3. It can be observed that the removal rates of Hg (II) and Cr (VI) decrease with an increase

**Table 1**
Comparison of the mechanical strength of ECH–CS–NZVI beads and P-NZVI.

| Beads | Stirring speed (rpm) | | | | |
|---|---|---|---|---|---|
| | 100 | 200 | 400 | 800 | 1200 |
| | Crumpling ratio (%) | | | | |
| ECH–CS–NZVI | 0 | 0 | 2 | 8 | 16 |
| P-NZVI | 0 | 0 | 0 | 0 | 1 |

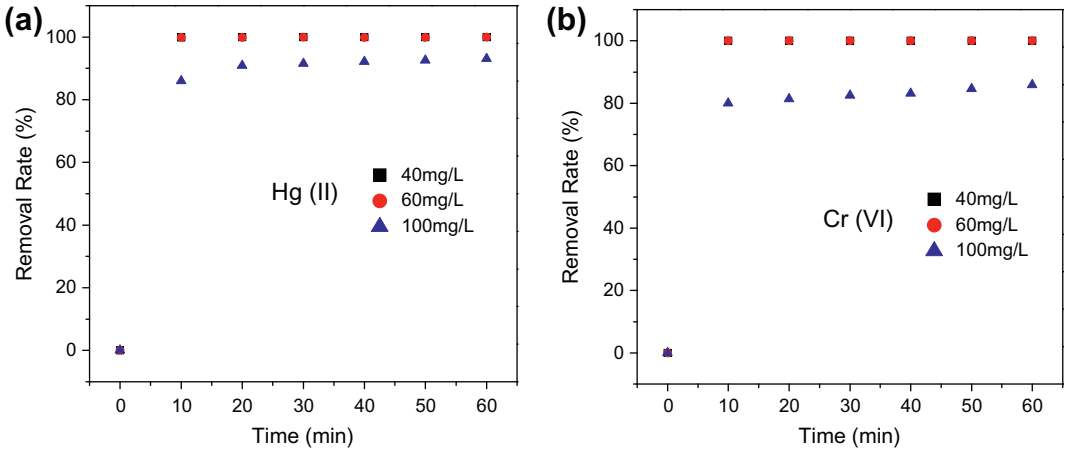


**Fig. 3.** Effect of concentrations of heavy metals on the removal of heavy metals by P-NZVI: (a) initial concentration of Hg (II): 40, 60 and 100 mg/L and (b) initial concentration of Cr (VI): 40, 60 and 100 mg/L. Error bars represent the standard deviation of the measurements.

of the initial concentrations of heavy metals. As a fixed P-NZVI dose, the total available adsorption sites are limited, thus, leading to a decrease in removal rate of heavy metals corresponding to an increased initial heavy metals concentration [29]. Similar results were also reported in other studies [5,12,14]. At the lower concentration (less than 60 mg/L), the removal rates of Hg (II) and Cr (VI) were all more than 99.8%. When the concentrations of Hg (II) and Cr (VI) were enhanced to 100 mg/L, the removal rates were 93.0% and 85.8% in an hour, respectively (Fig. 3(a) and (b)). At the same time, the removal capacity of Hg (II) and Cr (VI) by P-NZVI was 332.4 mg Hg/g Fe and 306.6 mg Cr/g Fe, respectively. The removal capacities obtained in the study are much higher than the results using commercial iron filings or other NZVI systems [19,25,30]. It is mainly attributed to the fact that pumice with highly porous and high surface areas was useful to adsorb heavy metals [17], leading to that heavy metals were accumulated on the surface or/and in the pores of pumice. Furthermore, pumice was useful to enhance the dispersibility of NZVI particles, thus, providing more reaction sites for heavy metals. As a result, P-NZVI went into effect by the cooperation of pumice and NZVI to remove more heavy metals.

The results indicated that P-NZVI was effective to remove various heavy metals in an hour, in terms of efficiency and speed, making it a promising candidate for applications to *in situ* environmental remediation, especially to the heavy metals pollution incidents with an extremely high concentration of heavy metals compared with the maximum concentrations allowed in groundwater [3].

### 3.5. Effect of pH

The pH of wastewater played an important role in removing of heavy metals. The dominant forms of heavy metals in aqueous solution were influenced by pH [31]. The solution pH can also affect the reaction rate of iron oxidation and corrosion of iron [32] and heavy metals can be removed through oxidation or/and complexation [33].

The effect of pH on the removal rates of heavy metals was investigated and the result is shown in Fig. 4. It can be seen that with an increase of pH from 3.11 to 8.13, the removal rates of Hg (II) are increased and all more than 99.1% in all conditions (Fig. 4(a)), while the removal rates of Cr (VI) are decreased gradually but all more than 96.0% (Fig. 4(b)). With increased hydroxyl groups, the surface of P-NZVI became dominantly negatively charged, leading to the enhanced attraction force between Hg (II) and P-NZVI. Therefore, the removal amount of Hg (II) was increased. The finding is in agreement with our previous work on other NZVI systems [25] and other researchers' work on the adsorption of heavy metals on pumice composite [16]. On the other hand, $HCrO_4^-$ predominates at pH between 1.0 and 6.0, and $CrO_4^{2-}$ pH above about 6.0 [31]. At lower pH, pumice was positively charged causing to form a dominantly positively charged surface of P-NZVI, while Cr (VI) existed mostly as an anion leading to the electrostatic attraction between Cr (VI) and P-NZVI [23,34]. As a result, Cr (VI) removal rate decreased with an increase of pH.

The removal rates of Hg (II) and Cr (VI) were all more than 96% (Fig. 4), indicating that these removal rates were not obviously affected by the solution pH. It may be contributed to the fact that the removal capacity of Hg (II) and Cr (VI) by P-NZVI is so high that the pH range in the study played only a small part in the removal rates of Hg (II) and Cr (VI).

### 3.6. P-NZVI reuse

The regeneration efficiency of P-NZVI was studied and the result is presented in Fig. 5. It is shown that a high removal rate can be maintained on the second, third and fourth runs. 87.8% and 62.3% of Hg (II) is removed on the second and third run, respectively (Fig. 5). Until the fourth time, the removal rate is still up to 56.7%. A similar trend is also found in Cr (VI) removal (Fig. 5). 76.7%, 56.7% and 45.5% of Cr (VI) is removed on the second, third and fourth run, respectively. The results suggest that P-NZVI is a regenerated material. Although other research reported that the process of removal of Cr(VI) by NZVI was irreversible [7], however, in our study, P-NZVI was washed by dilute HCl before being reused, which could dissolve Fe(III)–Cr(III) precipitate on the surface of NZVI [5,13,35]. As a result, fresh NZVI would be exposed to Hg (II) and Cr (VI) when P-NZVI was reused. Spent iron nanoparticles can be regenerated using renewable carbon materials at moderate temperature [36]. Fu et al. reported that the removal efficiencies of Cr (VI) were all above 80% and the resin-NZVI can be reused for many times [37]. By now, it can be concluded that extending utility time of P-NZVI makes it more practical in the *in situ* remediation of wastewater.

### 3.7. XPS characterization

The results of XPS characterization were shown in Figs. 6 and 7. It is clear that new peaks at the binding energy (BE) of 102.2 eV and 585.6 eV appeared after heavy metals reduction (Fig. 6(a) and (b)).

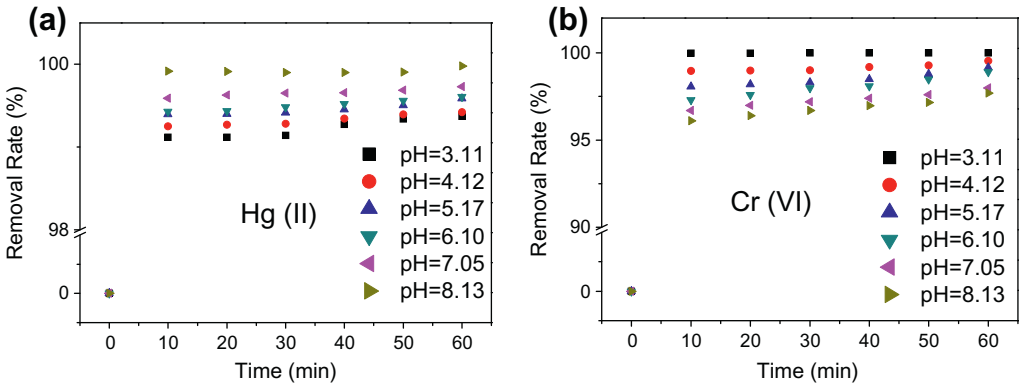


**Fig. 4.** Effect of pH value on the removal of heavy metals by P-NZVI. Initial concentration: (a) 60 mg/L Hg (II) and (b) 60 mg/L Cr (VI); the mass fraction of NZVI in P-NZVI: 7.7%, 0.28 g; temperature: 25 °C. Error bars represent the standard deviation of the measurements.

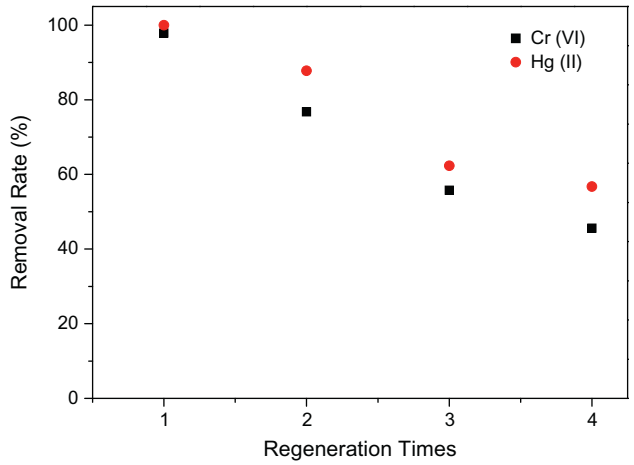


**Fig. 5.** Hg (II) and Cr (VI) removal efficiency in each cycle after regeneration using P-NZVI. Initial concentration: 60 mg/L Hg (II) and 60 mg/L Cr (VI); the mass fraction of NZVI in P-NZVI: 7.7%, 0.28 g; pH: 6.13; temperature: 25 °C; time: 1 h.

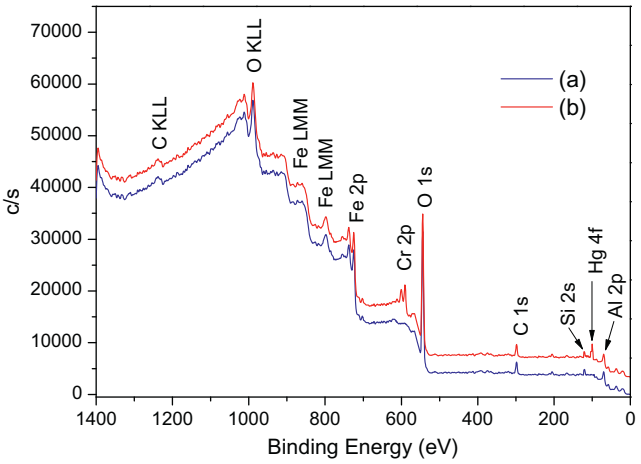


**Fig. 6.** Typical wide scan XPS spectra for P-NZVI before and after Hg (II) and Cr (VI) reduction: (a) before heavy metals reduction and (b) after heavy metals reduction. Initial Hg (II) and Cr (VI) concentration: 300 mg/L; the mass fraction of NZVI in P-NZVI: 7.7%, 0.28 g; pH: 6.13; temperature: 25 °C; time: 30 min.

The appearances of the bands were assigned to the photoelectron peak of Hg and Cr, respectively, which indicated the uptake of Hg and Cr on the surface of P-NZVI.

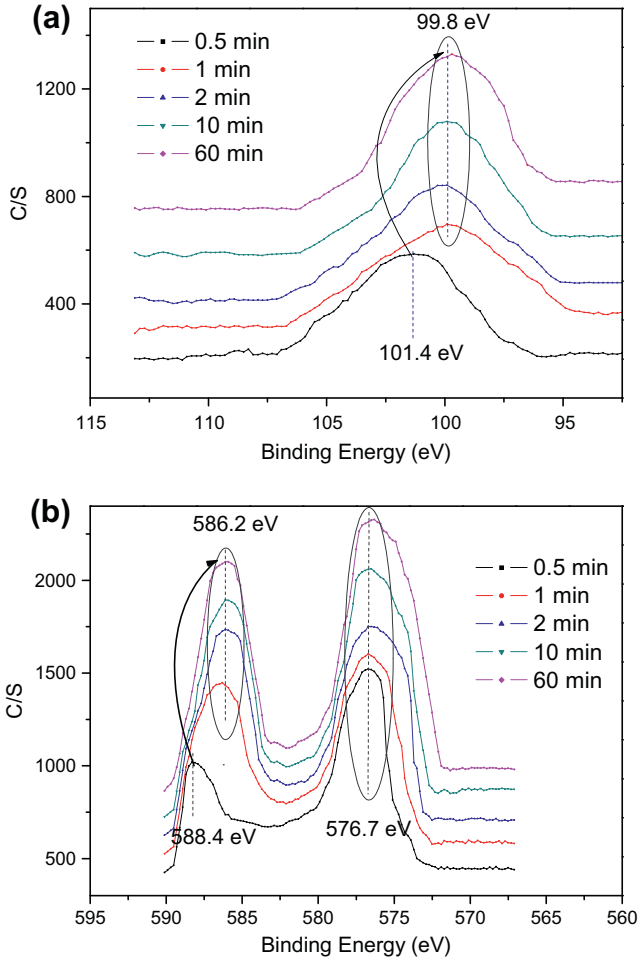


**Fig. 7.** High-resolution XPS survey of (a) Hg4f and (b) Cr2p of p-NZVI after reacting with wastewater. Initial Hg (II) and Cr (VI) concentration: 300 mg/L; the mass fraction of NZVI in P-NZVI: 7.7%, 0.28 g; pH: 6.13; temperature: 25 °C.

Detailed XPS surveys on the region of Hg4f and Cr2p are presented in Fig. 7. At 0.5 min, photoelectron peak centers at 101.4 eV (Fig. 7(a)), which has binding energies and line structures similar to those of Hg (II) [38]. Then, at 1, 2, 10 and 60 min, the photoelectron peak drifted and centered at 99.8 eV (Fig. 7(a)), which matched with the binding energy of Hg (0) [39]. The result indicated that an immediate physical adsorption of Hg (II) happened in the first 0.5 min before reduction of Hg (II) to Hg (0) by P-NZVI. The finding in the study proved the hypothesis that there

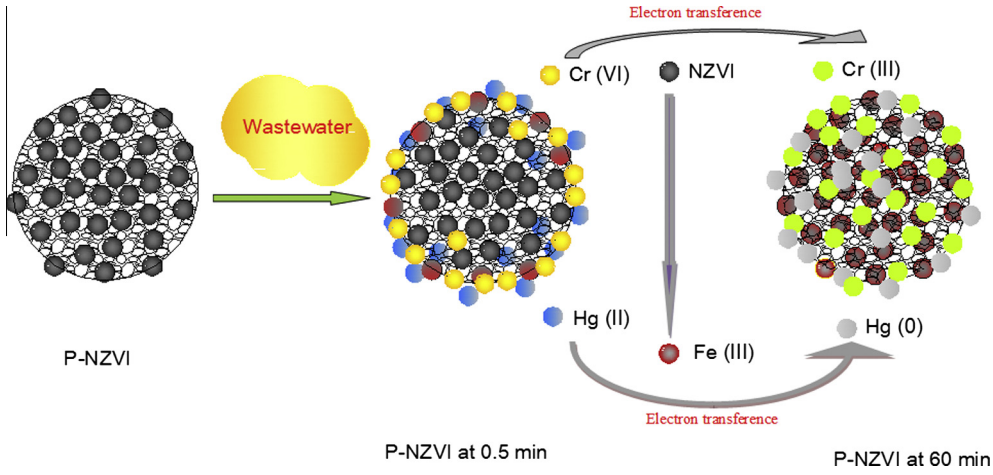


**Fig. 8.** A proposed mechanism (reactions + graphic) for Hg (II) and Cr (VI) reduction by P-NZVI.

might be a sorption of Hg (II) to NZVI prior to its reduction [35]. Sorption of Ni (II) onto NZVI was also observed as a proceeding step of surface reduction [40].

However, at 0.5 min, the $Cr2p_{3/2}$ and $Cr2p_{1/2}$ survey (Fig. 7(b)) presents photoelectron peaks centering at 576.7 and 588.4 eV, respectively, which come from Cr (III) and Cr (VI) [41] for $Cr_2O_3$ and $K_2CrO_4$ by analogy with other chromium compounds [42,43]. These binding energies are well in agreement with the results obtained by other researchers [41,44]. It is also observed that the peak at 576.7 eV is stronger than that at 588.4 eV, which means that a small of Cr (VI) are adsorbed on the P-NZVI surface and most of Cr (VI) is reduced to Cr (III). Then, the photoelectron peak for $Cr2p_{3/2}$ at 576.7 and 586.2 eV (Fig. 6(b)) was known as characteristics of Cr (III) [19,25] at 1, 2, 10 and 60 min. The XPS results implied that the reduction of Cr (VI) to Cr (III) was in effect for the removal of Cr (VI) after 0.5 min. The removal mechanism can be concluded that Cr (VI) was removed by a rapid physical adsorption in the first 0.5 min and predominantly by reduction. A mechanism for Hg (II) and Cr (VI) reduction by P-NZVI is proposed as shown in Fig. 8.

## 4. Conclusions

In this study, P-NZVI was successfully prepared with a higher capacity and efficiency to remove heavy metals from wastewater. Based on the results, the major findings are summarized as follows:

- NZVI particles are nearly spherical in shape with a mean diameter of 30.6 nm. NZVI particles are distributed uniformly on the surface of pumice demonstrating that pumice is effective to prevent NZVI particles from agglomerating. P-NZVI with a 7.7% NZVI mass fraction had a $S_{BET}$ of 32.2 $m^2/g$.
- The thermal stability of P-NZVI is good below 550 °C. The mechanical strength of P-NZVI is obviously enhanced using pumice as the support material.
- The removal rates of Hg (II) and Cr (VI) decrease with an increase of the initial concentrations of heavy metals.
- With an increase of pH from 3.11 to 8.13, the removal rates of Hg (II) are increased and all more than 99.1% in all conditions, while the removal rates of Cr (VI) are decreased gradually, but all more than 96.0%.
- P-NZVI is a regenerated material.
- The XPS results indicated that all of Hg (II) was reduced to Hg (0) while Cr (VI) was reduced to Cr (III) after 0.5 min, however, an immediate physical adsorption of Hg (II) and Cr (VI) happened in the first 0.5 min.

The results indicated that P-NZVI was effective to remove various heavy metals from wastewater, in terms of efficiency and speed, making it a promising candidate for applications to *in situ* environmental remediation.

## Acknowledgments

The authors thank Zhigang Zhang, Qian Wang and Fei He for their support with analyses. This work was financially supported by National Science & Technology Pillar Program (2012BAC07B00), Program for New Century Excellent Talents in University (NCET-10-0954), National Natural Science Foundation of China (21307090), the National Science & Technology Pillar Program (2012BAC07B02) and the University Science & Technology Development Project of Tianjin (20110528).

## References

[1] N.S. Bolan, D.C. Adriano, R. Natesan, B.-J. Koo, Effects of organic amendments on the reduction and phytoavailability of chromate in mineral soil, J. Environ. Qual. 32 (2003) 120–128.
[2] S.S. Beulah, K. Muthukumaran, Sorption studies of chromium (VI) and mercury (II) by high temperature activated carbon from *Syzygium Jambolanum* nut, E-J. Chem. 7 (2010) 299–307.
[3] General Administration of Quality Supervision, Inspection and Quarantine of the People's Republic of China (AQSIQ), Quality standard for groundwater (GB/T14848-93), 1993, pp. 2–3.
[4] A. Benhammou, A. Yaacoubi, L. Nibou, B. Tanouti, Study of the removal of mercury (II) and chromium (VI) from aqueous solutions by Moroccan stevensite, J. Hazard. Mater. B 117 (2005) 243–249.
[5] J.S. Cao, W.X. Zhang, Stabilization of chromium ore processing residue (COPR) with nanoscale iron particles, J. Hazard. Mater. 132 (2006) 213–219.
[6] S.R. Kanel, J.M. Greneche, H. Choi, Arsenic (V) removal from groundwater using nanoscale zero-valent iron as a colloidal reactive barrier material, Environ. Sci. Technol. 40 (2006) 2045–2050.
[7] L.N. Shi, X. Zhang, Z.L. Chen, Removal of chromium (VI) from wastewater using bentonite-supported nanoscale zero-valent iron, Water Res. 45 (2011) 886–892.
[8] L. Cumbal, J. Greenleaf, D. Leun, A.K. Sen-Gupta, Polymer supported inorganic nanoparticles: characterization and environmental applications, React. Funct. Polym. 54 (2003) 167–180.
[9] Z. Li, H. Kirk Jones, P. Zhang, R.S. Bowman, Chromate transport through columns packed with surfactant-modified zeolite/zero valent iron pellets, Chemosphere 68 (2003) 1861–1866.
[10] C. Uzum, T. Shahwan, A.E. Erolu, K.R. Hallam, T.B. Scott, I. Lieberwirth, Synthesis and characterization of kaolinite-supported zero-valent iron nanoparticles and their application for the removal of aqueous $Cu^{2+}$ and $Co^{2+}$ ions, Appl. Clay Sci. 43 (2009) 172–181.
[11] Y. Zhang, Y. Li, J. Li, L. Hu, X. Zheng, Enhanced removal of nitrate by a novel composite: nanoscale zero valent iron supported on pillared clay, Chem. Eng. J. 171 (2011) 526–531.
[12] B. Geng, Z. Jin, T. Li, X. Qi, Kinetics of hexavalent chromium removal from water by chitosan–$Fe^0$ nanoparticles, Chemosphere 75 (2009) 825–830.

[13] T. Liu, L. Zhao, D. Sun, X. Tan, Entrapment of nanoscale zero-valent iron in chitosan beads for hexavalent chromium removal from wastewater, J. Hazard. Mater. 184 (2010) 724–730.
[14] T. Liu, Z.L. Wang, L. Zhao, X. Yang, Enhanced chitosan/Fe0-nanoparticles beads for hexavalent chromium removal from wastewater, Chem. Eng. J. 189–190 (2012) 196–202.
[15] T. Candy, C.P. Sharma, Chitosan matrix for oral sustained delivery of ampicillin, Biomaterials 14 (1993) 939–944.
[16] M. Yavuz, F. Gode, E. Pehlivan, S. Ozmert, Y.C. Sharma, An economic removal of $Cu^{2+}$ and $Cr^{3+}$ on the new adsorbents: pumice and polyacrylonitrile/pumice composite, Chem. Eng. J. 137 (2008) 453–461.
[17] P. Catalfamo, I. Arrigo, P. Primerano, F. Corigliano, Efficiency of a zeolitized pumice waste as a low-cost heavy metals adsorbent, J. Hazard. Mater. B 134 (2006) 140–143.
[18] N. Moraci, P.S. Calabrò, Heavy metals removal and hydraulic performance in zero-valent iron/pumice permeable reactive barriers, J. Environ. Manage. 91 (2010) 2336–2341.
[19] S.M. Ponder, J.C. Darab, T.E. Mallouk, Remediation of Cr (VI) and Pb (II) aqueous solutions using supported, nanoscale zero-valent iron, Environ. Sci. Technol. 34 (2000) 2564–2569.
[20] L.D. Wesley, Determination of specific gravity and void ratio of pumice materials, Geotech. Test. J. 24 (2001) 418–422.
[21] A. Rachel, B. Lavedrine, M. Subrahmanyam, P. Boule, Use of porous lavas as supports of photocatalysts, Catal. Commun. 3 (2002) 165–171.
[22] K.V.S. Rao, A. Rachel, M. Subrahmanyam, P. Boule, Immobilization of $TiO_2$ on pumice stone for the photocatalytic degradation of dyes and dye industry pollutants, Appl. Catal. B 46 (2003) 77–85.
[23] M. Kitis, S.S. Kaplan, E. Karakaya, N.O. Yigit, G. Civelekoglu, Adsorption of natural organic matter from waters by iron coated pumice, Chemosphere 66 (2007) 130–138.
[24] M.D. Balaguer, M.T. Vicent, J.M. Paris, A comparison of different support materials in anaerobic fluidized bed reactors for the treatment of vinasse, Environ. Technol. 18 (1997) 539–544.
[25] T. Liu, X. Yang, Z.L. Wang, X. Yan, Enhanced chitosan beads-supported $Fe^0$-nanoparticles for removal of heavy metals from electroplating wastewater in permeable reactive barriers, Water Res. 47 (2013) 6691–6700.
[26] F.O. Akbal, N. Akdemir, A.N. Onar, FT-IR spectroscopic detection of pesticide after sorption onto modified pumice, Talanta 53 (2000) 131–135.
[27] X. Zhang, S. Lin, Z. Chen, M. Megharaj, R. Naidu, Kaolinite-supported nanoscale zero-valent iron for removal of $Pb^{2+}$ from aqeous solution: reactivity, characterization and mechanism, Water Res. 45 (2011) 3481–3488.
[28] T.Y. Guo, Y.Q. Xia, G.J. Hao, M.D. Song, B.H. Zhang, Adsorptive separation of hemoglobin by molecularly imprinted chitosan beads, Biomaterials 25 (2004) 5905–5912.
[29] T. Hiemstra, W.H. Van-Riemsdijk, Surface structural ion adsorption modeling of competitive binding of oxyanions by metal (hydr)oxides, J. Colloid Interface Sci. 210 (1999) 182–193.
[30] H. Genc-Fuhrman, P. Wu, Y.S. Zhou, A. Ledin, Removal of As, Cd, Cr, Cu, Ni and Zn from polluted water using an iron based sorbent, Desalination 226 (2008) 357–370.
[31] D. Mohan, C.U. Pittman, Activated carbons and low cost adsorbents for remediation of tri- and hexavalent chromium from water, J. Hazard. Mater. 137 (2006) 762–811.
[32] M.J. Alowitz, M.M. Scherer, Kinetics of nitrate, nitrite, and Cr (VI) reduction by iron metal, Environ. Sci. Technol. 36 (2002) 299–306.
[33] N. Melitas, O. Chuffe-Moscoso, J. Farrell, Kinetics of soluble chromium removal from contaminated water by zerovalent iron media: corrosion inhibition and passive oxide effects, Environ. Sci. Technol. 35 (2001) 3948–3953.
[34] V.M. Boddu, K. Abburi, J.L. Talbott, E.D. Smith, Removal of hexavalent chromium from wastewater using a new composite chitosan biosorbent, Environ. Sci. Technol. 37 (2003) 4449–4456.
[35] W. Yan, A.A. Herzing, C.J. Kiely, W.X. Zhang, Nanoscale zero-valent iron (nZVI): aspects of the core–shell structure and reactions with inorganic species in water, J. Contam. Hydrol. 118 (2010) 96–104.
[36] K.F. Chen, S. Li, W. Zhang, Renewable hydrogen generation by bimetallic zero valent iron nanoparticles, Chem. Eng. J. 170 (2011) 562–567.
[37] F. Fu, J. Ma, L. Xie, B. Tang, W. Han, S. Lin, Chromium removal using resin supported nanoscale zero-valent iron, J. Environ. Manage. 128 (2013) 822–827.
[38] J.J. Ehrhardt, P. Behra, P. Bonnissel-Gissinger, M. Alnot, R. Revel, XPS study of the sorption of Hg (II) onto pyrite $FeS_2$, Surf. Interface Anal. 30 (2000) 269–272.
[39] P. Behra, P. Bonnissel-Gissinger, M. Alnot, R. Revel, J.J. Ehrhardt, XPS and XAS study of the sorption of Hg (II) onto pyrite, Langmuir 17 (2001) 3970–3979.
[40] X. Li, W. Zhang, Iron nanoparticles: the core–shell structure and unique properties for Ni (II) sequestration, Langmuir 22 (2006) 4638–4642.
[41] B.A. Manning, J.R. Kiser, H. Kwon, S.R. Kanel, Spectroscopic investigation of Cr (III) and Cr (VI)-treated nanoscale zero-valent iron, Environ. Sci. Technol. 41 (2007) 586–592.
[42] L. Dambies, C. Guimon, S. Yiacoumi, E. Guibal, Characterization of metal ion interactions with chitosan by X-ray photoelectron spectroscopy, Colloid. Surf. A 177 (2001) 203–214.
[43] A.V. Naumkin, A. Kraut-Vass, S.W. Gaarenstroom and C.J. Powell, NIST X-ray Photoelectron Spectroscopy Database: NIST Standard Reference Database 20, Version 4.1, 2012.
[44] X.Q. Li, W.X. Zhang, Sequestration of metals cations with zerovalent iron nanoparticles – a study with high resolution X-ray photoelectron spectroscopy (HR-XPS), J. Phys. Chem. C 111 (2007) 6939–6946.